

Interspin interactions in ZnFe_2O_4 : Theoretical analysis of neutron scattering studyY. Yamada,¹ K. Kamazawa,² and Y. Tsunoda²¹*Advanced Research Center, Waseda University, 3-4-1 Ohkubo, Shinjuku-ku, Tokyo 169-8555, Japan*²*Department of Applied Physics, School of Science and Engineering, Waseda University, 3-4-1 Ohkubo, Shinjuku-ku, Tokyo 169-8555, Japan*

(Received 3 December 2001; published 1 August 2002)

We carried out a theoretical analysis of the recent neutron scattering study on ZnFe_2O_4 based on a simple classical Heisenberg spin model to elucidate the magnetic interactions in the system. The central issue is the possible frustration phenomena realized in the corner-shared tetrahedral arrangement of spins with an antiferromagnetic nearest-neighbor interaction. The results are summarized as follows: (i) From the diffuse intensity distributions in $(h k 0)$ - and $(h h 1)$ -zones, it is concluded that, contrary to the anticipation, the nearest-neighbor interaction is ferromagnetic, while the third-neighbor interaction is antiferromagnetic. (ii) From the shift of the peak position of the diffuse maximum as the temperature is varied, it is inferred that the ratio of the first- and the third-neighbor interactions $J_3/|J_1|$ is effectively temperature dependent. The value tends to be diminished at $T > 50$ K, which is consistent with the observation of a positive Curie-Weiss temperature deduced from the susceptibility measurement. (iii) From the systematic absence of the diffuse intensity around specific Bragg points, the lowest-energy “mode” of the spin-density fluctuations is characterized to be the “acoustic” mode.

DOI: 10.1103/PhysRevB.66.064401

PACS number(s): 75.10.Hk, 75.30.Et

I. INTRODUCTION

There are a number of magnetic materials belonging to different classes of crystal symmetry such as normal spinel, pyrochlore, and C15 Laves phase intermetallic compounds, which share a common feature in that the magnetic ions construct corner-shared tetrahedra as depicted in Fig. 1. If the interspin interaction in the system is assumed to be an antiferromagnetic interaction between nearest-neighbor spins, such a spin configuration provides physically a quite intriguing system of a so-called geometrical frustrated system.¹⁻⁴

Since Anderson¹ pointed out that the development of the spin long-range order in a frustrated system should be suppressed due to the degeneracy of the ground-state energy, both theoretical as well as experimental studies have been carried out extensively on such systems. Theoretically, several important concepts such as quantum spin liquid, spin ice, and topological spin glass have been recently proposed to characterize the ground state of the system.⁵⁻⁷ From a structural viewpoint, these ideas commonly postulate the existence of short-range antiferromagnetic clusters extending only to the size of a single tetrahedron. Experimentally, neutron scattering provides a powerful technique to investigate the magnetic structural behavior. In fact, the neutron-scattering studies on various types of crystals with corner-shared tetrahedra have confirmed the above prediction by observation of broad diffuse peaks even when extrapolated to 0 K.⁸⁻¹¹

ZnFe_2O_4 crystal belongs to normal spinel in which Fe^{3+} ions occupy solely the B site, thus forming the corner-shared tetrahedra of spins on Fe sites. It has been known that ZnFe_2O_4 has an extraordinarily low antiferromagnetic transition temperature ($T_N = 13$ K) as compared with similar classes of materials. Schiessl *et al.*¹² performed extensive studies on the magnetic properties of this substance. In particular, they observed the coexistence of short-range order with long-range order even below T_N by neutron-diffraction

measurement. From the diffuse scattering distribution the range of spin correlation is estimated to be 2.7 nm, which means that the system remains magnetically disordered, at least partly, even at the lowest-temperature observed ($T = 1.5$ K). Recently, Usa *et al.*¹³⁻¹⁶ have shown that the Bragg peaks corresponding to the partial long-range order become increasingly weaker in intensity and broader in full width at half maximum by a careful purifying procedure of the specimens, suggesting that the long-range order is driven by the quenched atomic disorder. This seems to allow the interpretation that ZnFe_2O_4 is an intrinsically frustrated spin system with nearest-neighbor antiferromagnetic interaction.

On the other hand, the measurement of static magnetic susceptibility¹⁷ $\chi(T)$ presents a somewhat puzzling feature: In typical materials characterized by the frustrated spin system such as YMn_2 (C15 Laves) and $\text{Y}_2\text{Mo}_2\text{O}_7$ (pyrochlore) the Curie-Weiss temperature θ_{CW} definitely give negative

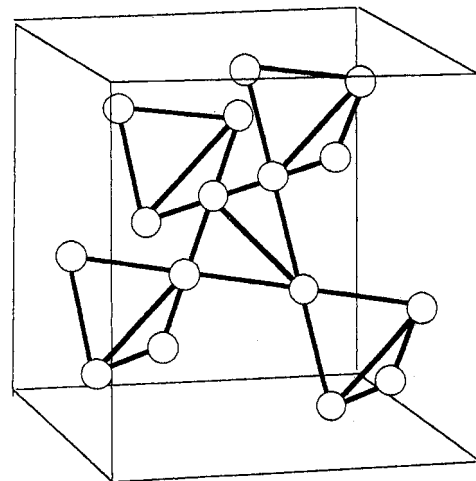


FIG. 1. The arrangement of B sites in the spinel structure, which is regarded as a network of corner-sharing tetrahedra.

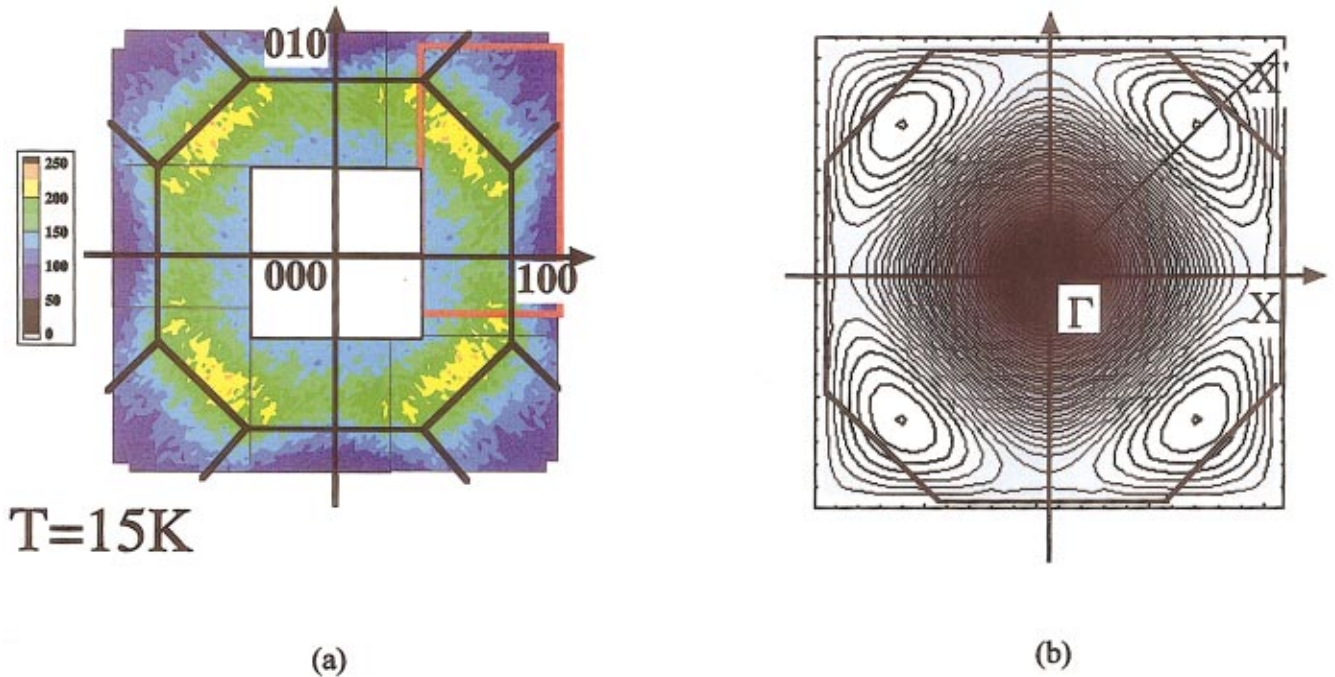


FIG. 2. (Color) (a) Observed distribution of the magnetic diffuse scattering at 15 K in the $(hk0)$ plane around the (000) reciprocal-lattice point. The ridge of strong diffuse intensity extends slightly inside the first Brillouin-zone boundary indicated by the thick lines. (b) Calculated intensity distribution corresponds to the experimental data shown in (a).

values, as it should in antiferromagnets.^{18,19} In contrast, θ_{CW} of ZnFe_2O_4 gives a positive value ($\theta_{CW} \approx 50$ K) when extrapolated using $\chi^{-1}(T)$ between $50 < T < 300$ K. Apparently, such a feature is in contradiction to the basic assumption of antiferromagnetic interaction between nearest neighbors in spin frustrated system.

Recently, Kamazawa *et al.*^{13,14,20} carried out detailed neutron-scattering experiments using single crystals of ZnFe_2O_4 . They mapped out the diffuse scattering intensity distributions in $(hk0)$ and $(hh1)$ planes at various temperatures, which provide information on the anisotropy of the spin correlations in the system. It is remarkable that the peak position of the diffuse scattering is located at the incommensurate \mathbf{q} value. Moreover, the diffuse intensities show systematic absence around the specific Bragg reflection. This characteristic feature gives information on the local spin arrangement in the form of a “structure factor” of the neutron spectrum.

It should also be remarked that the energy spectra of the diffuse scattering show that, in contrast to other frustrated systems, a large response is concentrated around the $\omega \cong 0$ regime to form the quasielastic scattering (Ref. 14). The energy width is within the energy resolution of the spectrometer utilized. Therefore the observed diffuse intensity is considered to be practically integrated over the ω direction, which means that the observed neutron magnetic diffuse scattering gives information on the instantaneous spin correlation on the static susceptibility $\chi(\mathbf{q})$.

The purpose of the present paper is to carry out a theoretical analysis of the results of the neutron scattering experiments presented by Kamazawa *et al.*, in order to elucidate

the nature of magnetic interactions to exhibit unique characteristic of the magnetic ordering process in the ZnFe_2O_4 crystal.

II. MODEL, CORRELATION, AND SCATTERING FUNCTION

To begin with, let us briefly reproduce some of the experimental results by Kamazawa *et al.* In Fig. 2(a), the diffuse scattering taken at $T = 15$ K is given, which shows a “ring-like” distribution in the $(hk0)$ plane. The high intensity region is lying slightly inside of the Brillouin-zone boundary lines of the fcc structure. As is clearly seen in Fig. 2(a), the maximum point is located at the incommensurate position given by $\mathbf{q}_0 = (0.70, 0.70, 0)$ at 15 K. It is also noticed that the \mathbf{q}_0 value shows strong temperature dependence so that $|\mathbf{q}_0|$ increases as the temperature is lowered.

Another important characteristic is that the diffuse intensities show systematic absence as the Bragg position is changed. As is typically demonstrated in Fig. 3(a) the diffuse scattering is almost absent in the Brillouin zone around the (220) reflection. Generally, the systematic absence in the $(hk0)$ zone follows the rule $h/2$: odd or $k/2$: odd. These are rather unique features to give unambiguous information on magnetic properties of ZnFe_2O_4 .

In order to carry out a theoretical analysis we assume the following simple classical Heisenberg spin model where the Hamiltonian is given by

$$H = \sum_{\alpha} \sum_{i,j} \sum_{\mu,\nu} J_{ij}^{\mu\nu} S_{i,\mu}^{\alpha} S_{j,\nu}^{\alpha} \quad (\mu, \nu = 1, 2, 3, 4, \quad \alpha = x, y, z), \quad (1)$$

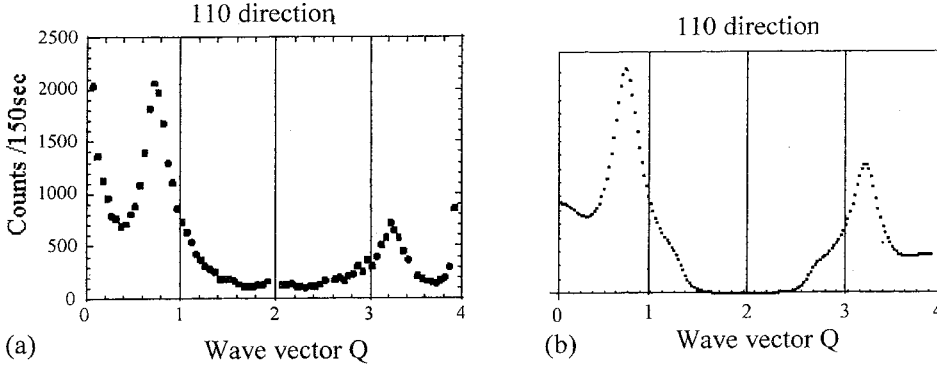


FIG. 3. (a) Observed profile of the diffuse intensity as scanned along the $[110]$ direction. (b) Calculated intensity profile corresponding to the experimental data, which clearly demonstrates the specific “extinction rule;” $h/2$: odd, $k/2$: odd.

where $S_{i,\mu}^\alpha$ is the α component of the spin vector at the μ th sublattice in the i th primitive rhombohedral unit cell. $J_{ij}^{\mu\nu}$ is the interaction parameter between the spin pairs, which is independent of the component index α .

We follow essentially the same procedure of the treatment developed by Reimers, Berlinsky, and Shi^{21,22} and later extended by Raju *et al.*²³ to include the dipolar interaction. We define the Fourier-transformed variable:

$$S_\mu^\alpha(\mathbf{q}) = \frac{1}{\sqrt{N}} \sum_i S_{i,\mu}^\alpha \exp(i\mathbf{q} \cdot \mathbf{r}_i). \quad (2)$$

Then the Hamiltonian is rewritten in the form

$$H = \sum_{\mathbf{q}} \sum_{\alpha} \mathbf{S}^{\alpha+}(\mathbf{q}) \cdot \mathbf{J}(\mathbf{q}) \cdot \mathbf{S}^\alpha(\mathbf{q}), \quad (3)$$

where $\mathbf{S}^\alpha(\mathbf{q})$ is the column vector with four components $S_1^\alpha(\mathbf{q})$, $S_2^\alpha(\mathbf{q})$, $S_3^\alpha(\mathbf{q})$, and $S_4^\alpha(\mathbf{q})$, and $J(\mathbf{q})$ is the 4×4 matrix whose (μ, ν) element is defined by

$$J^{\mu\nu}(\mathbf{q}) = \sum_j J_{ij}^{\mu\nu} \exp(i\mathbf{q} \cdot \mathbf{r}_{ij}). \quad (4)$$

Since the Hamiltonian is expressed by quadratic form, we obtain the normalized form:

$$H = \sum_{\alpha} \sum_{\mathbf{q}, \kappa} J^\kappa(\mathbf{q}) |\mathbf{S}_\kappa^\alpha(\mathbf{q})|^2 \quad (\kappa = 1, 2, 3, 4), \quad (5)$$

where $J^\kappa(\mathbf{q})$ is the energy eigenvalue belonging to the κ th branch, and $\mathbf{S}_\kappa^\alpha(\mathbf{q})$ is the corresponding normal coordinate given by the linear combination of $S_\mu^\alpha(\mathbf{q})$:

$$\mathbf{S}_\kappa^\alpha(\mathbf{q}) = \sum_{\mu} C_\mu^\kappa(\mathbf{q}) S_\mu^\alpha(\mathbf{q}). \quad (6)$$

Within a random-phase approximation (RPA) treatment, one of the diagonal elements of the static susceptibility tensor is given by

$$\chi(\mathbf{q}) = \sum_{\kappa} \frac{\chi^0(T)}{1 - J^\kappa(\mathbf{q})\chi^0(T)}, \quad (7)$$

where $\chi^0(T)$ is the susceptibility without any interaction, which is explicitly given, in the case of the Heisenberg spin with $|\mathbf{S}| = 1$, by

$$\chi^0(T) = \frac{1}{3k_B T}. \quad (8)$$

The long-range order develops below the critical transition temperature given by

$$T_c = \frac{J^\lambda(q_0)}{3k_B}, \quad (9)$$

where $J^\lambda(q_0)$ is the lowest-energy eigenvalue specified by the wave vector \mathbf{q}_0 and the branch index λ .

The neutron scattering cross section associated with the spin fluctuations in the vicinity of the phase transition is given by

$$I(\mathbf{K}) = \sum_{i,j} \sum_{\mu,\nu} \langle [\mathbf{S}_i - \kappa(\mathbf{S}_i \cdot \kappa)] \cdot [\mathbf{S}_j - \kappa(\mathbf{S}_j \cdot \kappa)] \rangle \times \exp[i\mathbf{K} \cdot (\mathbf{r}_i^\mu - \mathbf{r}_j^\nu)], \quad (10)$$

$$= \frac{2}{3} \frac{\chi^0(T)}{1 - J^\lambda(\mathbf{q})\chi^0(T)} |F^\lambda(\mathbf{K})|^2, \quad (11)$$

$$\mathbf{q} = \mathbf{K} - \mathbf{K}_h, \quad \kappa = \mathbf{K}/|\mathbf{K}|, \quad (12)$$

where $\mathbf{K}_h = h\mathbf{a}^* + k\mathbf{b}^* + l\mathbf{c}^*$ is the Bragg position ($h k l$) nearest to the scattering vector \mathbf{K} . $F^\lambda(\mathbf{K})$ is the structure factor corresponding to the λ th branch which is given explicitly by

$$F^\lambda(\mathbf{K}) = \sum_{\mu} C_\mu^\lambda(\mathbf{q}) \exp[i\mathbf{K} \cdot \mathbf{r}^\mu], \quad (13)$$

where \mathbf{r}^μ is the position vector of the μ th Fe- ion drawn from the origin of the unit cell.

III. ANALYSIS OF EXPERIMENTAL DATA

It is informative to plot the energy dispersion of the lowest-lying branch, $J^\lambda(\mathbf{q})$, in the reciprocal space in frustrated systems to investigate the degeneracy of the ground-state energy. In the case of corner-shared tetrahedral with nearest-neighbor interaction, the dispersion is completely flat within the $(h k 0)$ zone, as was first pointed out by Reimers, Berlinsky, and Shi.^{21,22} (See Fig. 4.)

Since the observed neutron scattering intensity [Fig. 2(a)] shows definite modulation within the $(h k 0)$ zone, we infer

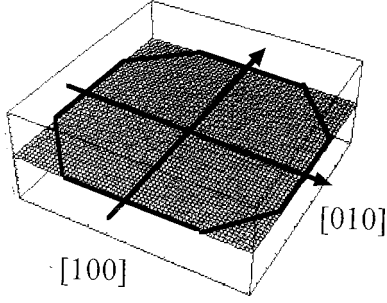


FIG. 4. The energy eigenvalues of the lowest-lying branch in the $(hk0)$ reciprocal plane when only the nearest-neighbor antiferromagnetic interaction is taken into account. The flat dispersion indicates the strong frustration effect occurring in the corner-sharing tetrahedral arrangement of the spins.

that, at least in the framework of the present model (isotropic Heisenberg spin model), the nearest-neighbor antiferromagnetic-type interaction is certainly inadequate to describe the ordering process of ZnFe_2O_4 . The possible further interactions up to third neighbors are listed in Table I. It should be remarked that there are two different exchange paths to connect third neighbors, so that there are a total of four parameters, J_1 , J_2 , J_3 , and J'_3 .

Instead of carrying out a numerical fitting procedure including these interaction parameters simultaneously, we check the individual properties of $J^\lambda(\mathbf{K})$ for each interaction parameter. We find out that $J^\lambda(\mathbf{K})$ for J_3 shows ringlike energy contours, which are quite reminiscent of the observed intensity distribution. (See Fig. 5.) Therefore, in order to reduce the number of disposable parameters, we satisfy ourselves by taking J_1 and J_3 into account.

In order to investigate the properties of the spin correlation, or the static susceptibility, we momentarily neglect the effect of the structure factor and put

$$I(\mathbf{K}) \propto \frac{\chi^0(T)}{1 - J^\lambda(\mathbf{q})\chi^0(T)},$$

$$\mathbf{q} = \mathbf{K} - \mathbf{K}_h \quad (14)$$

within the Brillouin zone around an arbitrary Bragg point \mathbf{K}_h . Using Eq. (9), the above equation is rewritten in more physically transparent form:

TABLE I. List of the n th nearest-neighbor Fe^{3+} pairs up to $n=4$ and their possible exchange paths via anions (x) and A- or B-site metals. There are two different exchange paths for the third neighbors.

	d	Z	Exchange path	\mathbf{J}
Nearest neighbor	$\sqrt{2}$	6	B_0-B_1, B_0-X-B_1	J_1
Second-nearest neighbor	$\sqrt{6}$	12	$B_0-X-A-X-B_2$	J_2
Third-nearest neighbor	$\sqrt{8}$	6	$B_0-X-B_1-X-B_3, B_0-X-A-X-B_3$	J'_3, J_3
Fourth-nearest neighbor	$\sqrt{10}$	12	$B_0-X-A-X-B_4$	J_4

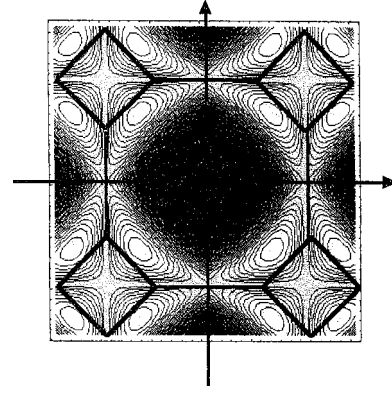


FIG. 5. The contour map of the energy eigenvalue of the lowest-lying branch when only the third-neighbor antiferromagnetic interaction is taken into account. The pattern is reminiscent of the observed diffuse intensity distribution given in Fig. 2(a).

$$I(\mathbf{K}) \propto \frac{1}{\Delta + [J^\lambda(\mathbf{q}) - J^\lambda(\mathbf{q}_0)]}, \quad (15)$$

$$\Delta = k_B(T - T_c). \quad (16)$$

Using Eq. (15), we calculate $I(\mathbf{K})$ and compare with the experimental intensity distribution taken around $(0\ 0\ 0)$ at $T=15$ K, where J_3/J_1 is left as the adjustable parameter.

We have found that the overall agreement of the pattern is obtained only when J_1 is taken to be ferromagnetic ($J_1 < 0$) and J_3 is antiferromagnetic ($J_3 > 0$). The best-fit distribution is obtained at $J_3/J_1 = -1.33$, shown in Fig. 2(b). As is seen in the figure, the overall characteristic of the distribution of $I(\mathbf{K})$ in the $(0\ 0\ 0)$ Brillouin zone is well reproduced. Especially the highest peak position is situated at the incommensurate point of $\mathbf{q}_0 = (0.70, 0.70, 0)$ which is in good agreement with the observed \mathbf{q}_0 value.

The experimental $|\mathbf{q}_0|$ value shows appreciable temperature dependence as depicted in Fig. 6. Starting from $q_0 = 0.75\sqrt{2}a^*$ at 1.5 K, the $|\mathbf{q}_0|$ value decreases as the temperature is increased, until it finally becomes obscured at $q_0 \sim 0.45\sqrt{2}a^*$ at $T \cong 30$ K. In the present treatment, the temperature dependence of q_0 can only be explained as being due to the temperature variation of the effective interaction parameters. In Fig. 7, we plot the temperature variation of

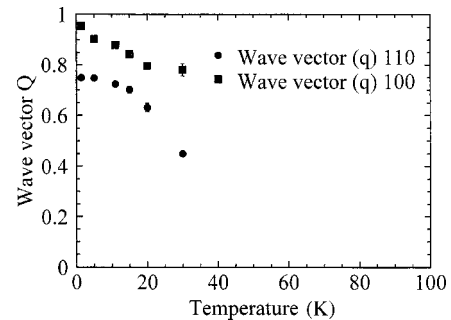


FIG. 6. Observed temperature dependence of the peak positions of the diffuse intensity on $[110]$ and $[100]$ directions. The peak along the $[110]$ direction become obscured at $T \cong 30$ K as it becomes influenced by the tail of the strong Bragg peak at (000) .

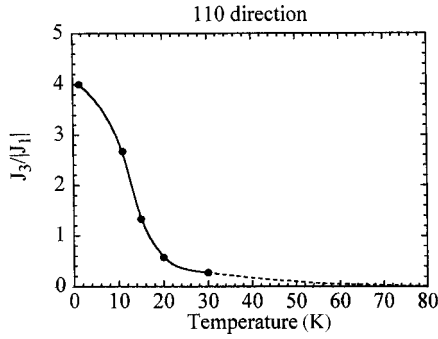


FIG. 7. Calculated temperature dependence of the ratio J_3/J_1 deduced from the observed temperature dependence of the peak position given in Fig. 6.

the J_3/J_1 value as obtained from the observed q_0 value. It is noticed that at $T \sim 50$ K, the system is effectively described by the ferromagnetic nearest-neighbor interaction ($J_1 < 0, J_3 \sim 0$), which is consistent with the susceptibility measurements to give a positive Curie-Weiss temperature. It is also noticed that the value of $|J_3/J_1|$ sharply increases at $T < 15$ K, reaching 4.0 at 1.5 K. This seems to be quite an extraordinary situation since the third-neighbor interaction would be usually an order-of-magnitude weaker as compared with the nearest-neighbor interaction. This point will be discussed later.

So far, we have only discussed the energy eigenvalue $J^\lambda(\mathbf{q})$. We now turn to the problem of the spatial configuration of the spins in the unit cell which is directly manifested in the properties of the structure factor of the spin-density wave (SDW) given by Eq. (13). We first calculate the components of the normal coordinate $\{C_\mu^\lambda(\mathbf{q})\}$ for each sublattice, some of which at the representative points in \mathbf{q} space are listed in Table II. As is given in the Appendix, it is shown that the structure factor for the lowest-lying branch $F^\lambda(\mathbf{K})$ is approximately expressed by

$$F^\lambda(\mathbf{K}) \propto \sum_{\mu} \exp(i\mathbf{K}_h \cdot \mathbf{r}^\mu), \quad (17)$$

TABLE II. The components of the eigenvectors $C_\mu^\lambda(\xi, \xi, 0)$ of the lowest-energy branch at the representative points in the range $0 \leq \xi \leq 1.0$.

hkl	μ			
	1	2	3	4
0 0 0	0.500 0	0.500 0	0.500 0	0.500 0
0.1 0.1 0	0.486 76+0.077 09 <i>i</i>	0.486 76+0.077 09 <i>i</i>	0.526 80	0.526 80
0.2 0.2 0	0.448 59+0.145 76 <i>i</i>	0.448 59+0.145 76 <i>i</i>	0.507 07	0.507 07
0.3 0.3 0	0.390 52+0.198 98 <i>i</i>	0.390 52+0.198 98 <i>i</i>	0.554 89	0.554 89
0.4 0.4 0	0.320 74+0.233 03 <i>i</i>	0.320 74+0.233 03 <i>i</i>	0.585 51	0.585 51
0.5 0.5 0	0.248 07+0.248 07 <i>i</i>	0.248 07+0.248 07 <i>i</i>	0.613 94	0.613 94
0.6 0.6 0	0.178 54+0.245 74 <i>i</i>	0.178 54+0.245 74 <i>i</i>	0.638 54	0.638 54
0.7 0.7 0	0.114 77+0.225 26 <i>i</i>	0.114 77+0.225 26 <i>i</i>	0.660 37	0.660 37
0.8 0.8 0	0.058 80+0.180 96 <i>i</i>	0.058 80+0.180 96 <i>i</i>	0.681 02	0.681 02
0.9 0.9 0	0.0165 92+0.104 761 <i>i</i>	0.0165 92+0.104 761 <i>i</i>	0.699 11	0.699 11
1 1 0	0	0	0.707 11	0.707 11

irrespective of the value \mathbf{q} in the Brillouin zone around \mathbf{K}_h . Equation (17) clearly shows that there exists the extinction rule (systematic absence) concerning the diffuse intensity around the reciprocal-lattice points satisfying ($h/2$: odd or $k/2$: odd) in the ($h k 0$) zone, which is consistent with the observed results. The comparison of the calculated value of $I(\mathbf{K})$ along the $[110]$ direction throughout (0 0 0) to (4 4 0) with the observed intensity profile is given in Figs. 3(a) and 3(b).

For later discussions, we take notice that, in analogy to the phonons (lattice distortion wave), the lowest-lying branch in the present spin system may be called the ‘‘acoustic’’ branch of the spin-density wave modes in which the spin densities on different sublattices can be described simply by a single coherent wave propagating through the whole lattice:

$$S_{i,\mu}^\alpha = \hat{S}^\alpha \exp(i\mathbf{q} \cdot \mathbf{r}_i^\mu), \quad (18)$$

so that all spins on the four sublattices are arranged ‘‘in phase’’ as $\mathbf{q} \rightarrow 0$:

$$C_{(\mathbf{q}=0)}^\lambda = \frac{1}{2}(1, 1, 1, 1). \quad (19)$$

IV. SUMMARY AND DISCUSSIONS

Summarizing, we have analyzed the reported neutron scattering results on ZnFe₂O₄ based on a simple classical Heisenberg spin model in order to elucidate the magnetic interactions in the system, a central issue being the apparent frustration in the corner-shared tetrahedral spin arrangement. The results are summarized as follows.

(i) From the diffuse intensity distributions in ($h k 0$) and ($h h 1$) zones, it is concluded that, contrary to the anticipation, the nearest-neighbor interaction is ferromagnetic, while the third-neighbor interaction is antiferromagnetic. (ii) From the shift of the peak position of the diffuse maximum as the temperature is varied, it is inferred that the ratio $|J_3/J_1|$ is effectively temperature dependent, which tends to be diminished at $T > 50$ K. (iii) From the systematic absence of the diffuse intensity around specific Bragg points, the lowest-

energy “mode” of the spin-density fluctuations is characterized to be the “acoustic” mode.

Recently, Ballou, Lelièvre-Berna, and Fák carried out a neutron scattering investigation on a C15-type frustrated system ($Y_{0.97}Sc_{0.03}Mn_2$ (Ref. 9)). It is interesting to notice that the intensity profile scanned along the $[\xi \ \xi \ 0]$ direction through $\xi=0$ to $\xi=4$ [the same scan as given in Fig. 3(a)] gives a completely opposite systematic absence to the present case: diffuse intensities are absent around (0 0 0) and (4 4 0) and are present around (2 2 0). (See Fig. 2 of Ref. 9.) This implies that the lowest-lying branch of the spin-fluctuation mode in the YMn_2 system is the “optical” mode with the eigenvector $C_{(q=0)}^\lambda = \frac{1}{2}(1, 1, -1, -1)$, which is consistent with the fact that ($Y_{0.97}Sc_{0.03}Mn_2$) is an intrinsic frustrated system with the antiferromagnetic nearest-neighbor interaction.

Kanamori developed an extensive theoretical investigation on various types of exchange interactions based on the symmetry properties of the relevant orbitals.²⁴ We follow the arguments for the case of the $Fe^{3+}-O-Fe^{3+}$ exchange path in a 90° configuration corresponding to the present system. The dominant superexchange interaction is due to the one between the $d\gamma$ orbitals hybridized with $p\sigma$ orbitals of the anion, which acts ferromagnetically because of the orthogonality of the Wannier functions. However, there are other mechanisms which tend to act antiferromagnetically, such as $d\gamma-d\epsilon$ (hybridized with either $p\sigma$ or $p\pi$ orbitals), or $d\gamma-d\gamma$ (hybridized with a $3s$ orbital) exchange paths. In addition, there is the possibility of the direct exchange interaction, which also contributes to the antiferromagnetic interaction. In the present system, it would not be unreasonable to consider that the resultant nearest-neighbor interaction is only barely ferromagnetic due to the cancellation between these competitive interactions. In fact, the experimental results on various compounds with $Fe^{3+}-X-Fe^{3+}$ in a 90° configuration as summarized by Motida and Miyahara show that the nearest-neighbor interactions fall into the region around $J \sim 0$ (Ref. 25).

Moreover, it is known that the direct exchange interaction is very sensitive to the metal-metal distance, so that the antiferromagnetic direct exchange interaction increases as the metal-metal distance is contracted as the temperature is lowered, which means an even more effective cancellation of the nearest-neighbor interaction at lower temperatures. Such features are consistent, at least qualitatively, with the observed temperature variation of $|J_3/J_1|$ as given in Fig. 7.

Within the RPA of a classical Heisenberg spin system, one expects that the system should attain the long-range order of the spin-density wave state with the incommensurate wave vector \mathbf{q}_0 at a finite temperature T_c given by Eq. (9). Actually, however, a pure $ZnFe_2O_4$ system does not attain the long-range order at the lowest-temperature observed (4.2 K). It is seen that along the ringlike low-energy “ditch,” $J(q)$ is almost degenerated, the maximum energy difference being 11% of the full energy dispersion of the lowest branch. There will still be a number of SDW states with different q values attainable by thermal fluctuation of the system even at 4 K.

ACKNOWLEDGMENT

We would like to thank Professor K. Kohn of Waseda University for supplying us with a $ZnFe_2O_4$ single-crystal specimen for the neutron scattering measurements.

APPENDIX

We calculate the neutron scattering intensity $I(\mathbf{K})$,

$$I(\mathbf{K}) = \sum_{i,j} \sum_{\mu,\nu} \langle [S_i^\mu - \kappa(S_i \cdot \kappa)] \cdot [S_j^\nu - \kappa(S_j \cdot \kappa)] \rangle \times \exp[i\mathbf{K} \cdot (\mathbf{r}_i^\mu - \mathbf{r}_j^\nu)], \quad (A1)$$

$$\mathbf{r}_i^\mu = \mathbf{r}_i + \mathbf{r}^\mu, \quad (A2)$$

where \mathbf{r}_i^μ is the position vector of the μ th Fe ion in the i th primitive unit cell. We consider the spin fluctuations due to the spin-density waves belonging to the lowest-lying branch λ , which is expressed by

$$S_\mu^\alpha = \langle \hat{S}_\lambda^\alpha \rangle C_\mu^\lambda(\mathbf{q}) \exp(i\mathbf{q} \cdot \mathbf{r}_i), \quad (A3)$$

where $\langle \hat{S}_\lambda^\alpha \rangle$ is the amplitude of the SDW and $C_\mu^\lambda(\mathbf{q})$ is the μ th component of the four-dimensional vector $\mathbf{C}^\lambda(\mathbf{q})$.

At a glance of the calculated components of $\mathbf{C}^\lambda(\mathbf{q})$ ($\mathbf{q} \parallel [110]$) for the lowest-lying branch (see Table II), we can easily see that $C_\mu^\lambda(\mathbf{q})$ is approximately given by

$$C_\mu^\lambda(\mathbf{q}) \cong e^{i\mathbf{q} \cdot \mathbf{r}^\mu}, \quad (A4)$$

from which the SDW is simply expressed by a single coherent wave throughout the four sublattices:

$$S_{i,\mu}^\alpha \cong \langle \hat{S}_\lambda^\alpha \rangle e^{i\mathbf{q} \cdot \mathbf{r}_i^\mu}. \quad (A5)$$

Substituting Eqs. (A5) into (A1), it is easily shown that

$$I(\mathbf{K}) = |F^\lambda(\mathbf{K})|^2 |\langle \hat{S}_\lambda^\alpha(\mathbf{q}) \rangle|^2, \quad (A6)$$

$$F^\lambda(\mathbf{K}) \cong \sum_{\mu} e^{i\mathbf{K}_h \cdot \mathbf{r}^\mu}. \quad (A7)$$

Notice that $F^\lambda(\mathbf{K})$ is dependent only on the value \mathbf{K}_h , the Bragg position nearest to the scattering vector, irrespective of the value of \mathbf{q} in the first Brillouin zone around \mathbf{K}_h . This indicates that there is a definite extinction rule concerning the diffuse intensity. By inserting the position vectors \mathbf{r}^μ for Fe ions, the extinction rule results in $F^\lambda(\mathbf{K}) \cong 0$ when $h/2$: odd or $k/2$: odd for $(h, k, 0)$.

- ¹P. W. Anderson, Phys. Rev. **102**, 1008 (1956).
- ²C. L. Henley, J. Appl. Phys. **61**, 3962 (1987).
- ³J. N. Reimers, Phys. Rev. B **45**, 7287 (1992).
- ⁴M. J. P. Gingras, C. V. Stager, N. P. Raju, B. D. Gaulin, and J. E. Greedan, Phys. Rev. Lett. **78**, 947 (1997).
- ⁵M. P. Zinkin and M. J. Harris, J. Magn. Magn. Mater. **140–144**, 1803 (1995).
- ⁶B. Canals and C. Lacroix, Phys. Rev. Lett. **80**, 2933 (1998).
- ⁷S. T. Bramwell and M. J. Harris, J. Phys.: Condens. Matter **10**, L215 (1998).
- ⁸M. J. Harris, S. T. Bramwell, D. F. McMorrow, T. Zeiske, and K. W. Godfrey, Phys. Rev. Lett. **79**, 2554 (1997).
- ⁹R. Ballou, E. Lelièvre-Berna, and B. Fåk, Phys. Rev. Lett. **76**, 2125 (1996).
- ¹⁰S.-H. Lee, C. Broholm, T. H. Kim, W. Ratcliff II, and S.-W. Cheong, Phys. Rev. Lett. **84**, 3718 (2000).
- ¹¹J. S. Gardner, B. D. Gaulin, S.-H. Lee, C. Broholm, N. P. Raju, and J. E. Greedan, Phys. Rev. Lett. **83**, 211 (1999).
- ¹²W. Schiessl, W. Potzel, H. Karzel, M. Steiner, G. M. Kalvius, A. Martin, M. K. Krause, I. Halevy, J. Gal, W. Schäfer, G. Will, M. Hillberg, and R. Wäppling, Phys. Rev. B **53**, 9143 (1996).
- ¹³K. Kamazawa, Y. Tsunoda, K. Odaka, and K. Kohn, J. Phys. Chem. Solids **60**, 1261 (1999).
- ¹⁴K. Kamazawa, H. Kadowaki, Y. Tsunoda, and K. Kohn (unpublished).
- ¹⁵T. Usa, K. Kamazawa, S. Nakamura, H. Sekiya, Y. Tsunoda, K. Kohn, and M. Tanaka, in *Proceedings of the Eighth International Conference on Ferrite*, Kyoto, Japan, 2000, edited by M. Abe and Y. Yamazaki, p. 316.
- ¹⁶T. Usa, K. Kamazawa, S. Nakamura, H. Sekiya, Y. Tsunoda, K. Kohn, and M. Tanaka (unpublished).
- ¹⁷Yu. G. Chukalkin and V. R. Shtirts, Fiz. Tverd. Tela (Leningrad) **30**, 2919 (1988) [Sov. Phys. Solid State **30**, 1683 (1988)].
- ¹⁸M. Shiga, K. Fujisawa, and H. Wada, J. Phys. Soc. Jpn. **62**, 1329 (1993).
- ¹⁹N. P. Raju, E. Gmelin, and R. K. Kremer, Phys. Rev. B **62**, 12 167 (1992).
- ²⁰K. Kamazawa, Y. Tsunoda, K. Odaka, and K. Kohn, *Proceedings of the Eighth International Conference on Ferrite*, Kyoto, Japan, 2000, edited by M. Abe and Y. Yamazaki, p. 217.
- ²¹J. N. Reimers, A. J. Berlinsky, and A.-C. Shi, Phys. Rev. B **43**, 865 (1991).
- ²²J. N. Reimers, Phys. Rev. B **46**, 193 (1992).
- ²³N. P. Raju, M. Dion, M. J. P. Gingras, T. E. Mason, and J. E. Greedan, Phys. Rev. B **59**, 14 489 (1999).
- ²⁴J. Kanamori, J. Phys. Chem. Solids **10**, 87 (1959).
- ²⁵K. Motida and S. Miyahara, J. Phys. Soc. Jpn. **28**, 1188 (1970).